

## A WAY TO IMPROVE THE ACCURACY OF DISPLACEMENT MEASUREMENT BY A TWO-PROBE IMPLEMENTATION OF MICROWAVE INTERFEROMETRY

Aleksei V. Doronin, Nikolai B. Gorev\*,  
Inna F. Kodzhespirova, and Evgeny N. Privalov

Department for Functional Elements of Control Systems, Institute of Technical Mechanics, National Academy of Sciences of Ukraine, 15 Leshko-Popel St., Dnepropetrovsk 49005, Ukraine

**Abstract**—This paper addresses the possibility of displacement measurement by microwave interferometry at an unknown reflection coefficient with the use of as few as two probes. The case of an arbitrary interprobe distance is considered. The measurement error as a function of the interprobe distance is analyzed with the inclusion of variations of the detector currents from their theoretical values. The analysis has shown that as the interprobe distance decreases, the maximum measurement error passes through a minimum for reflection coefficients close to unity and increases monotonically for smaller reflection coefficients. Based on the results of the analysis, the interprobe distance is suggested to be one tenth of the guided operating wavelength  $\lambda_g$ . In comparison with the conventional interprobe distance of  $\lambda_g/8$ , the suggested one offers a marked reduction in the maximum measurement error for reflection coefficients close to unity, while for smaller ones this error remains much the same (for a detector current error of 3%, the maximum measurement error in percent of the operating wavelength is 2.2% and 1.0% at  $\lambda_g/10$  as against 4.8% and 2.7% at  $\lambda_g/8$  for a reflection coefficient of 1 and 0.9, respectively, and 2.9% at  $\lambda_g/10$  as against 2.4% at  $\lambda_g/8$  for a reflection coefficient of 0.1).

---

*Received 5 February 2013, Accepted 9 April 2013, Scheduled 11 April 2013*

\* Corresponding author: Nikolai B. Gorev (gorev57@mail.ru).

## 1. INTRODUCTION

Microwave interferometry is widely used for position sensing [1, 2] and displacement measurement [3]. This is due to its ability to provide fast noncontact measurements, applicability to dusty or smoky environments (as distinct from laser Doppler sensors [4–6] or vision-based systems using digital image processing techniques [7]), and simple hardware implementation in comparison with other microwave measuring instruments such as, for example, the step-frequency continuous-wave radar sensor [8]. Interferometric sensors also have a relatively faster system response time than other types of sensors due to the fact that they are generally operated with a single-frequency source.

Interferometry is basically a phase-sensitive detection process capable of resolving any measured physical quantity within a fraction of the operating wavelength. In displacement measurements, the displacement of a moving object (target) is extracted from the phase shift between the signal reflected from the target and the reference signal. This phase shift can be determined from two quadrature signals. At present, the usual way to form such signals is to use special hardware incorporating a power divider and a phase-detecting processor, which is an analog [3] or a digital [9] quadrature mixer. In doing so, measures have to be taken to minimize the nonlinear phase response of the quadrature mixer, which is caused by its phase and amplitude unbalances.

In our previous paper [10], we reported a displacement measurement technique in which the quadrature signals are extracted from the outputs of two probes placed in a waveguide section one eighth of the guided operating wavelength  $\lambda_g$  apart. Its hardware implementation is far simpler than that of conventional techniques based on quadrature mixing [3, 9], and its distinctive feature is the possibility of displacement measurement at an unknown reflection coefficient with two probes, while since the classic text by Tischer [11] it has been universally believed that at least three probes are needed to determine or eliminate the unknown reflection coefficient. The reduction in the number of probes simplifies the design of the measuring waveguide section and alleviates the problem of interprobe interference. Theoretically, the technique reported in [10] gives the exact value of the displacement for reflection coefficients (at the location of the probes) no greater than  $1/\sqrt{2}$  and in the general case determines it to a worst-case accuracy of about 4.4% of the operating wavelength. The aim of this paper is to show that this accuracy can be improved by using an interprobe distance other than the conventional

$\lambda_g/8$ . This aim is achieved by extending the approach proposed in [10] to the case of an arbitrary interprobe distance.

## 2. MODEL OF TWO-PROBE MEASUREMENTS

Consider two probes, 1 and 2, with square-law semiconductor detectors placed  $l$  apart in a waveguide section between a microwave oscillator and a target so that probe 1 is farther from the target (Fig. 1).

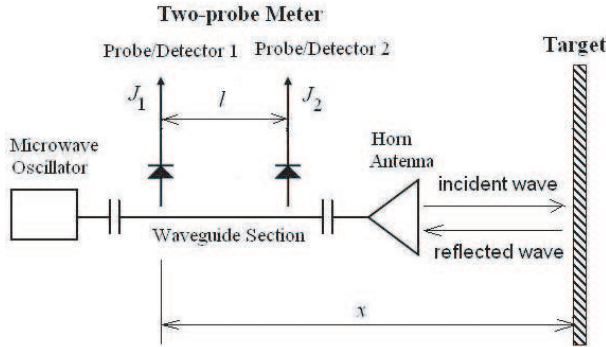


**Figure 1.** Schematic of two-probe measurements.

In this case, the detector currents  $J_1$  and  $J_2$  (normalized to their values in the absence of a reflected wave, which have to be determined prior to displacement measurements, for example, using a matched load) are

$$J_1 = 1 + |\Gamma|^2 + 2 |\Gamma| \cos \psi, \tag{1}$$

$$J_2 = 1 + |\Gamma|^2 + 2 |\Gamma| \sin (\psi - \beta) \tag{2}$$

where  $|\Gamma|$  and  $\psi$  are the magnitude and phase of the unknown complex reflection coefficient  $\Gamma = |\Gamma|e^{i\psi}$  at the location of probe 1, i.e.,  $\psi$  is the phase difference between the reflected and the incident wave at that point,  $\beta = \frac{\pi}{2}(\frac{l-\lambda_g/8}{\lambda_g/8})$ , and the subscripts “1” and “2” refer to probes 1 and 2, respectively (for simplicity, in the following discussion the magnitude of the complex reflection coefficient will be referred to as the reflection coefficient).

The phase difference  $\psi$  may be written as

$$\psi = \frac{4\pi x}{\lambda_0} + \phi \tag{3}$$

where  $x$  is the distance between the target and probe 1,  $\lambda_0$  the free-space operating wavelength, and the term  $\phi$ , which is governed by

the waveguide section and horn antenna geometry and the phase shift caused by the reflection, does not depend on the distance  $x$ .

Let it be desired to find the displacement  $\Delta x(t)$  of the target relative to its initial position  $x(t_0)$  from the measured currents  $J_1(t)$  and  $J_2(t)$ . This displacement can be unambiguously determined from the quadrature signals  $\cos \psi$  and  $\sin \psi$ . From Eqs. (1) and (2) we have

$$\cos \psi = \frac{a_1 - |\Gamma|^2}{2|\Gamma|}, \quad (4)$$

$$\sin \psi = \frac{a_2 + a_1 \sin \beta - |\Gamma|^2 (1 + \sin \beta)}{2|\Gamma| \cos \beta} \quad (5)$$

where

$$a_1 = J_1 - 1, \quad a_2 = J_2 - 1. \quad (6)$$

Combining the squares of Eqs. (4) and (5) gives the biquadratic equation in  $|\Gamma|$

$$|\Gamma|^4 - [a_1 + a_2 + 2(1 - \sin \beta)] |\Gamma|^2 + \frac{a_1^2 + a_2^2 + 2a_1 a_2 \sin \beta}{2(1 + \sin \beta)} = 0. \quad (7)$$

This equation has two positive roots

$$|\Gamma|_1 = \left[ \frac{a_1 + a_2}{2} + 1 - \sin \beta + \sqrt{\left( \frac{a_1 + a_2}{2} + 1 - \sin \beta \right)^2 - \frac{a_1^2 + a_2^2 + 2a_1 a_2 \sin \beta}{2(1 + \sin \beta)}} \right]^{1/2}, \quad (8)$$

$$|\Gamma|_2 = \left[ \frac{a_1 + a_2}{2} + 1 - \sin \beta - \sqrt{\left( \frac{a_1 + a_2}{2} + 1 - \sin \beta \right)^2 - \frac{a_1^2 + a_2^2 + 2a_1 a_2 \sin \beta}{2(1 + \sin \beta)}} \right]^{1/2}, \quad (9)$$

one of which is extraneous.

Denote the positive extraneous root by  $|\Gamma|_{ext}$ . Using Eqs. (4) and (5), the absolute term of Eq. (7) can be brought to the form

$$\frac{a_1^2 + a_2^2 + 2a_1 a_2 \sin \beta}{2(1 + \sin \beta)} = |\Gamma|^2 \{ |\Gamma|^2 + 2|\Gamma| [\cos \psi + \sin(\psi - \beta)] + 2(1 - \sin \beta) \} \quad (10)$$

whence we have

$$|\Gamma|_{ext} = \left\{ |\Gamma|^2 + 2|\Gamma| [\cos \psi + \sin(\psi - \beta)] + 2(1 - \sin \beta) \right\}^{1/2}. \quad (11)$$

A simple analysis shows that for  $|\Gamma| \leq \sqrt{\frac{1-\sin\beta}{2}} \equiv |\Gamma|_0$  the extraneous root  $|\Gamma|_{ext}$  will always be greater than or equal to  $|\Gamma|$ , and thus the reflection coefficient  $|\Gamma|$  will always be given by  $|\Gamma|_2$  because  $|\Gamma|_2 \leq |\Gamma|_1$ . For  $|\Gamma| > |\Gamma|_0$ , the extraneous root  $|\Gamma|_{ext}$  will be smaller than  $|\Gamma|$  if  $\sin(\psi + \beta_0) < -|\Gamma|_0/|\Gamma|$  where  $\beta_0 = \arcsin |\Gamma|_0$ , and thus the reflection coefficient will be given by  $|\Gamma|_1$  if  $\sin(\psi + \beta_0) < -|\Gamma|_0/|\Gamma|$ , otherwise it will be given by  $|\Gamma|_2$ . For clarity, all these cases are summarized in Table 1.

**Table 1.** The roots  $|\Gamma|_1$  and  $|\Gamma|_2$  of Eq. (7).

$ \Gamma  \leq  \Gamma _0$	$ \Gamma  >  \Gamma _0$	
	$\sin(\psi + \beta_0) < - \Gamma _0/ \Gamma $	$\sin(\psi + \beta_0) \geq - \Gamma _0/ \Gamma $
$ \Gamma _1 =  \Gamma _{ext}$	$ \Gamma _1 =  \Gamma $	$ \Gamma _1 =  \Gamma _{ext}$
$ \Gamma _2 =  \Gamma $	$ \Gamma _2 =  \Gamma _{ext}$	$ \Gamma _2 =  \Gamma $

In the case  $|\Gamma| \leq |\Gamma|_0$ , the reflection coefficient  $|\Gamma|$  is unambiguously determined from Eq. (7) as its root  $|\Gamma|_2$ , which allows one to find  $\cos\psi$  and  $\sin\psi$  from Eqs. (4) and (5). The displacement of the target can readily be extracted from  $\cos\psi$  and  $\sin\psi$  using the phase unwrapping method, which is a powerful tool to resolve the phase ambiguity problem in a variety of applications [3, 12, 13]. Specifically, the displacement  $\Delta x$  of the target at time  $t_n$ ,  $n = 0, 1, 2, \dots$ , from its initial position  $x(t_0)$  can be found by the following phase unwrapping algorithm [14]

$$\varphi(t_n) = \begin{cases} \arctan \frac{\sin \psi(t_n)}{\cos \psi(t_n)}, & \sin \psi(t_n) \geq 0, \cos \psi(t_n) \geq 0, \\ \arctan \frac{\sin \psi(t_n)}{\cos \psi(t_n)} + \pi, & \cos \psi(t_n) < 0, \\ \arctan \frac{\sin \psi(t_n)}{\cos \psi(t_n)} + 2\pi, & \sin \psi(t_n) < 0, \cos \psi(t_n) \geq 0, \end{cases} \quad (12)$$

$$\Delta\varphi(t_n) = \varphi(t_n) - \varphi(t_{n-1}), \quad (13)$$

$$\theta(t_n) = \begin{cases} 0, & n = 0, \\ \theta(t_{n-1}) + \Delta\varphi(t_n), & |\Delta\varphi(t_n)| \leq \pi, \quad n = 1, 2, \dots, \\ \theta(t_{n-1}) + \Delta\varphi(t_n) - 2\pi \operatorname{sgn}[\Delta\varphi(t_n)], & |\Delta\varphi(t_n)| > \pi, \quad n = 1, 2, \dots, \end{cases} \quad (14)$$

$$\Delta x(t_n) = \frac{\lambda_0}{4\pi} \theta(t_n), \quad n = 0, 1, 2, \dots, \quad (15)$$

where  $\varphi$  and  $\theta$  are the wrapped and unwrapped phases, respectively.

In the case  $|\Gamma| > |\Gamma|_0$ , the root  $|\Gamma|_2$  will not always be equal to  $|\Gamma|$ , but, as will be shown below, the displacement can also be determined to sufficient accuracy using the root  $|\Gamma|_2$  as the reflection coefficient. As discussed above, the root  $|\Gamma|_2$  will be extraneous for  $\sin(\psi + \beta_0) < -|\Gamma|_0/|\Gamma|$ . In terms of the wrapped phase  $\varphi$ , this condition becomes

$$\varphi_1 < \varphi < \varphi_2 \quad (16)$$

where

$$\varphi_1 = \pi + \arcsin \frac{|\Gamma|_0}{|\Gamma|} - \beta_0, \quad \varphi_2 = 2\pi - \arcsin \frac{|\Gamma|_0}{|\Gamma|} - \beta_0. \quad (17)$$

The phase error  $\Delta\varphi_{er}$  introduced when the extraneous root is taken as the reflection coefficient will be

$$\Delta\varphi_{er} = \begin{cases} \varphi_{ap} - \varphi + 2\pi & \text{if } 0 \leq \varphi_{ap} \leq \pi/2 \quad \text{and } 3\pi/2 \leq \varphi < 2\pi, \\ \varphi_{ap} - \varphi - 2\pi & \text{if } 3\pi/2 \leq \varphi_{ap} < 2\pi \quad \text{and } 0 \leq \varphi \leq \pi/2, \\ \varphi_{ap} - \varphi & \text{otherwise} \end{cases} \quad (18)$$

where  $\varphi$  is the actual wrapped phase;  $\varphi_{ap}$  is the apparent wrapped phase calculated by Eqs. (4), (5), and (12) with the extraneous root  $\{|\Gamma|^2 + 2|\Gamma|[\cos\psi + \sin(\psi - \beta)] + 2(1 - \sin\beta)\}^{1/2}$  in place of  $|\Gamma|$ ;  $2\pi$  is added or subtracted to overcome the  $2\pi$ -discontinuity problem at the boundary between the first and the fourth quadrant.

As can be seen from Eqs. (13)–(15), the displacement error is governed only by the phase error at the initial and the current measurement point because the intermediate points cancel one another. Because of this, the maximum displacement error will be

$$\Delta x_{er \max} = \frac{\lambda_0}{4\pi} (\Delta\varphi_{er \max} - \Delta\varphi_{er \min}) \quad (19)$$

where  $\Delta\varphi_{er \max}$  and  $\Delta\varphi_{er \min}$  are the maximum and the minimum value of the function  $\Delta\varphi_{er}(\varphi)$  on the interval  $0 \leq \varphi < 2\pi$ .

### 3. ADVISABLE INTERPROBE DISTANCE

Figure 2 shows the ratio  $\Delta x_{er \max}/\lambda_0 = (\Delta\varphi_{er \max} - \Delta\varphi_{er \min})/4\pi$  versus  $|\Gamma|$  for different values of the interprobe distance:  $l = \lambda_g/8$ ,  $l = 0.9(\lambda_g/8) = 9\lambda_g/80$ ,  $l = 0.8(\lambda_g/8) = \lambda_g/10$ ,  $l = 0.7(\lambda_g/8) = 7\lambda_g/80$ , and  $l = 0.5(\lambda_g/8) = \lambda_g/16$ . As illustrated, the error  $\Delta x_{er \max}$  decreases rapidly with decreasing  $l$ . However, in actual practice the interprobe distance cannot be decreased below a certain lower limit. First, too small interprobe distances are difficult to realize technically, which is due in particular to the fact that any probe has a finite size. Second, as the interprobe distance decreases, the detector currents approach each

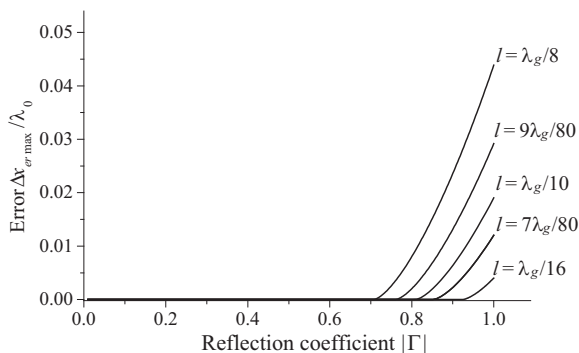


**Figure 2.** Maximum displacement error  $\Delta x_{er\ max}$  versus the reflection coefficient  $|\Gamma|$  at different values of the interprobe distance  $l$  when the only source of error is the use of the root  $|\Gamma|_2$  where it is extraneous.

other, thus increasing the contribution of the error component caused by variations of the detector currents from their theoretical values given by Eqs. (1) and (2) (such variations may be due to the effect of the reflecting surface shape and orientation and the antenna radiation pattern on the reflected wave, electromagnetic noise, etc.). As a result, at some value of the interprobe distance the error may pass through a minimum and start increasing. Because of this, calculations were conducted to find out an advisable value of the interprobe distance. In the calculations, the determination of the relative displacement of a target executing a harmonic vibratory motion was simulated. In doing so, variations of the detector currents from their theoretical values were modeled by random current noise. The distance  $x$  of the target to probe 1 and the detector currents  $J_1$  and  $J_2$  were simulated as

$$x(t) = x_0 + A \sin(2\pi t/T), \tag{20}$$

$$\psi = \psi_0 + \frac{4\pi}{\lambda_0} A \sin(2\pi t/T), \quad \psi_0 = \phi + \frac{4\pi x_0}{\lambda_0}, \tag{21}$$

$$J_1 = \left(1 + |\Gamma|^2 + 2|\Gamma| \cos \psi\right) (1 + A_n r), \tag{22}$$

$$J_2 = [1 + |\Gamma|^2 + 2|\Gamma| \sin(\psi - \beta)] (1 + A_n r)$$

where  $t$  is the time;  $A$  and  $T$  are the target vibration amplitude and period;  $x_0$  and  $\psi_0$  are the distance  $x$  and the phase  $\psi$  at  $t = 0$ ;  $A_n$  is the noise amplitude;  $r$  is a random variable uniformly distributed between  $-1$  and  $1$ .

The calculations were conducted for different values of the interprobe distance  $l$  and the reflection coefficient  $|\Gamma|$  at  $A = 2.5\lambda_0$  and

$A_n = 0.03$ . To get the maximum possible error, the initial phase  $\psi_0$  should be such that  $\Delta\varphi_{er}(\psi_0) = \Delta\varphi_{er\min}$  or  $\Delta\varphi_{er\max}$ ; for definiteness,  $\psi_0$  was chosen such that  $\Delta\varphi_{er}(\psi_0) = \Delta\varphi_{er\min}$ .

Figure 3 shows the maximum displacement error  $\Delta x_{er\max}$  (normalized to the free-space wavelength  $\lambda_0$ ) over five cycles of vibration versus the interprobe distance  $l$  (normalized to  $\lambda_g/8$ ) at different values of the reflection coefficient  $|\Gamma|$ . As illustrated, with decreasing interprobe distance the error passes through a minimum for reflection coefficients close to unity ( $|\Gamma| = 1, 0.95$ , and  $0.9$ ) and increases monotonically for smaller reflection coefficients ( $|\Gamma| = 0.7, 0.3, 0.2$ , and  $0.1$ ). The nonmonotonicity of the error has been discussed above. Its monotonic increase is due to the fact that for  $|\Gamma| < |\Gamma|_0$  (for  $l \leq \lambda_g/8$ ,  $|\Gamma|_{0\min} = 1/\sqrt{2} = 0.707$ ) the displacement error is governed only by variations of the detector currents from their theoretical values. As can be seen from the figure,  $l = 0.8(\lambda_g/8) = \lambda_g/10$  may be chosen as an advisable interprobe distance because at this value of  $l$ , in comparison with  $l = \lambda_g/8$ , the error shows a more than two-fold decrease for reflection coefficients close to unity while remaining much the same for smaller ones.

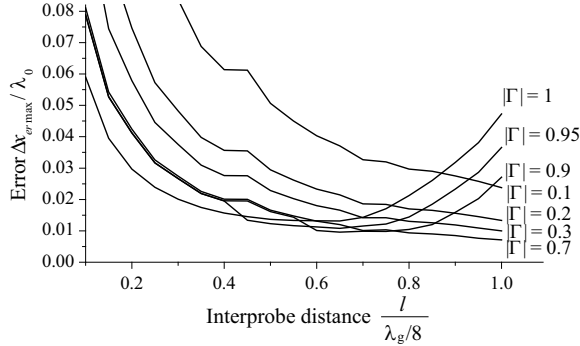


**Figure 3.** Maximum displacement error  $\Delta x_{er\max}$  versus the interprobe distance  $l$  at different values of the reflection coefficient  $|\Gamma|$  when the error is due both to the use of the root  $|\Gamma|_2$  where it is extraneous and to detector current noise.

#### 4. EXPERIMENTAL VERIFICATION

To cover the cases of both small and near-unity reflection coefficients, free-space and waveguide measurements were made using the two-probe measuring setup described in [10]. In the experiments, the

interprobe distance remained fixed, and the ratio  $l/\lambda_g$  was varied by varying the microwave oscillator frequency. Two frequencies were used: 9.7 and 8.7 GHz, at which  $l = \lambda_g/8$  and  $\lambda_g/10$ , respectively. The reflection coefficient was determined from Eq. (7) as its root  $|\Gamma|_2$ .

In the free-space measurements, the target was a  $\varnothing 218$  mm brass disc put in motion by an electrically driven crank mechanism. The disc peak-to-peak amplitude  $2A$  (twice the crank radius) was 10 cm, and the minimum distance between the disc and the antenna was 58 cm. The results for 9.7 and 8.7 GHz are presented in Figs. 4 and 5, respectively. The figures show the measured disc displacement (a), the disc peak-to-peak amplitude error  $\Delta_{2A} = |2A_{meas} - 2A_{act}|$  (b), and the measured reflection coefficient. As can be seen from the figures, the measured reflection coefficient is less than  $|\Gamma|_{0\min} = 1/\sqrt{2} = 0.707$ . So the root  $|\Gamma|_2$  gives the actual reflection coefficient. As is evident from the graphs, for these small values of the reflection coefficient the error  $\Delta_{2A}$  at 8.7 GHz ( $l = \lambda_g/10$ ) does not increase much in comparison with 9.7 GHz ( $l = \lambda_g/8$ ).

It can also be seen from the graphs that the measured reflection

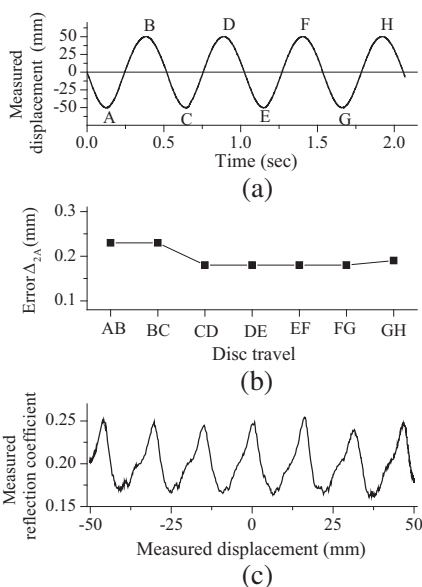


**Figure 4.** Free-space measurements: (a) measured disc displacement, (b) peak-to peak amplitude error, and (c) measured reflection coefficient at 9.7 GHz ( $l = \lambda_g/8$ ).

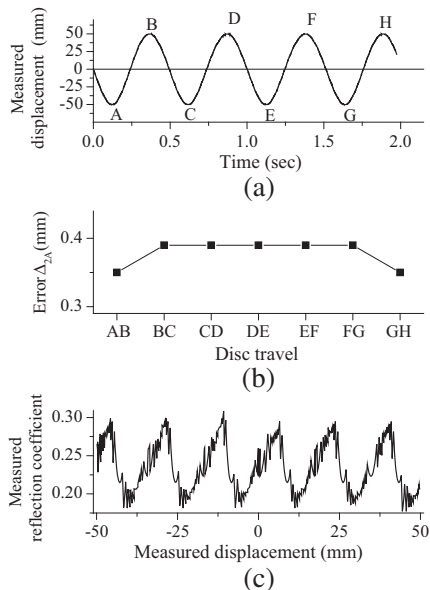


**Figure 5.** Free-space measurements: (a) measured disc displacement, (b) peak-to peak amplitude error, and (c) measured reflection coefficient at 8.7 GHz ( $l = \lambda_g/10$ ).

coefficient oscillates with a period equal to the half-wavelength ( $\lambda_0/2 = 15.5$  mm at 9.7 GHz and 17.2 mm at 8.7 GHz). Such a behavior of the reflection coefficient is indicative of the presence of multi-reflections between the antenna and the disc surface. However, at the location of the probes (in the waveguide section between the microwave oscillator and the antenna, see Fig. 1) only two waves are present: the incident wave and the reflected wave. Thus Eqs. (1) and (2) hold in the presence of multi-reflections between the antenna and the target surface too. Clearly these multi-reflections affect the amplitude of the reflected wave in the waveguide section, but in the proposed technique their effect is accounted for by determining the instantaneous value of the reflection coefficient.

In the waveguide measurements, a short-circuiting piston was mounted at the end of the waveguide section with the probes in place of the horn antenna used in the free-space measurements. The displacement was measured as the piston was moved every 1 mm. The results for 9.7 GHz ( $l = \lambda_g/8$ ) and 8.7 GHz ( $l = \lambda_g/10$ ) are presented in Fig. 6. The figure shows the measured piston displacement (a), the

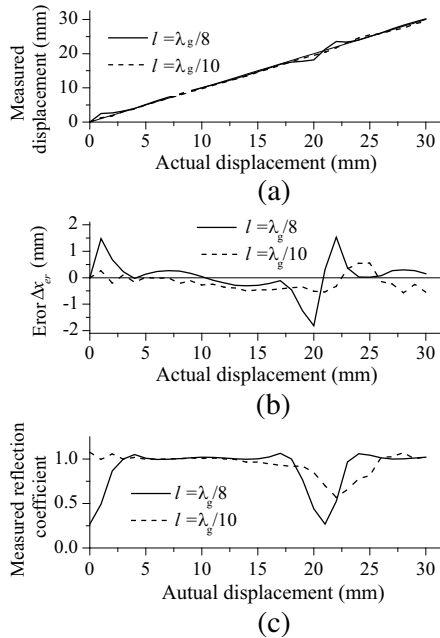


**Figure 6.** Waveguide measurements: (a) measured piston displacement, (b) displacement error, and (c) measured reflection coefficient at 9.7 GHz ( $l = \lambda_g/8$ ) and 8.7 GHz ( $l = \lambda_g/10$ ).

displacement error  $\Delta x_{er} = \Delta x_{meas} - \Delta x_{act}$  (b), and the measured reflection coefficient (c). The measured reflection coefficient shows near-unity plateaus and valleys. The plateaus correspond to the actual reflection coefficient, and the valleys occur where the root  $|\Gamma|_2$  becomes extraneous, which also manifests itself as the increase in the displacement error observed at the location of the valleys. The maximum displacement error decreases from 1.8 mm at  $l = \lambda_g/8$  (4.3% of  $\lambda_g = 4.18$  cm) to 0.6 mm at  $l = \lambda_g/10$  (1.2% of  $\lambda_g = 5.21$  cm). The decrease in the displacement error in this case (a near-unity reflection coefficient) is much greater than its increase in the case of a small reflection coefficient discussed above.

## 5. CONCLUSION

It is shown that the displacement of a target with an unknown reflection coefficient can be determined to within a few percent of the operating wavelength using a two-probe implementation of microwave interferometry and the measurement error can be reduced by using an interprobe distance shorter than the conventional one eighth of the guided operating wavelength  $\lambda_g$ . The interprobe distance is suggested to be  $\lambda_g/10$ . At this suggested value, in comparison with  $\lambda_g/8$ , the inherent error of two-probe measurements, which manifests itself at reflection coefficients close to unity, is reduced, while the error introduced by variations of the detector currents from their theoretical values, which increases as the interprobe distance and/or the reflection coefficient decrease, remains much the same. So the major advantage of the two-probe technique proposed in this paper over that proposed in [10] is a distinctly smaller measurement error at near-unity reflection coefficients.

## REFERENCES

1. Stezer, A., C. G. Diskus, K. Lubke, and H. W. Thim, "Microwave position sensor with sub millimeter accuracy," *IEEE Transactions on Microwave Theory and Techniques*, Vol. 47, No. 12, 2621–2624, 1999.
2. Benlarbi-Delai, A., D. Matton, and Y. Leroy, "Short-range two-dimension positioning by microwave cellular telemetry," *IEEE Transactions on Microwave Theory and Techniques*, Vol. 42, No. 11, 2056–2062, 1994.
3. Kim, S. and C. Nguyen, "A displacement measurement technique using millimeter-wave interferometry," *IEEE Transactions on*

- Microwave Theory and Techniques*, Vol. 51, No. 6, 1724–1728, 2003.
4. Cunha, A. and E. Caetano, “Dynamic measurements on stay cables of stay-cable bridges using an interferometry laser system,” *Experimental Techniques*, Vol. 23, No. 3, 38–43, 1999.
  5. Kaito, K., M. Abe, and Y. Fujino, “Development of a non-contact scanning vibration measurement system for real-scale structures,” *Structure and Infrastructure Engineering*, Vol. 1, No. 3, 189–205, 2005.
  6. Mehrabi, A. B., “In-service evaluation of cable-stayed bridges, overview of available methods, and findings,” *Journal of Bridge Engineering*, Vol. 11, No. 6, 716–724, 2006.
  7. Lee, J. J. and M. Shinozuka, “A vision-based system for remote sensing of bridge displacement,” *NDT & E International*, Vol. 39, No. 5, 425–431, 2006.
  8. Gentile, C., “Application of microwave remote sensing to dynamic testing of stay-cables,” *Remote Sensing*, Vol. 2, No. 1, 36–51, 2010.
  9. Kim, S. and C. Nguyen, “On the development of a multifunction millimeter-wave sensor for displacement sensing and low-velocity measurement,” *IEEE Transactions on Microwave Theory and Techniques*, Vol. 52, No. 11, 2503–2512, 2004.
  10. Doronin, A. V., N. B. Gorev, I. F. Kodzhespoirova, and E. N. Privalov, “Displacement measurement using a two-probe implementation of microwave interferometry,” *Progress In Electromagnetics Research C*, Vol. 32, 245–258, 2012.
  11. Tischer, F. J., *Mikrowellen-Messtechnik*, Springer-Verlag, Berlin, 1958.
  12. Chavez, S., Q.-S. Xiang, and L. An, “Understanding phase maps in MRI: A new cutline phase unwrapping method,” *IEEE Transactions on Medical Imaging*, Vol. 21, No. 8, 966–977, 2002.
  13. Hasar, U. C., J. J. Barroso, C. Sabah, and Y. Kaya, “Resolving phase ambiguity in the inverse problem of reflection-only measurement methods,” *Progress In Electromagnetics Research*, Vol. 129, 405–420, 2012.
  14. Silvia, M. T. and E. A. Robinson, *Deconvolution of Geophysical Time Series in the Exploration for Oil and Natural Gas*, Elsevier Scientific Publishing Company, Amsterdam, Oxford, New York, 1979.